Modulation and Vectorial Summation of the Spinalized Frog's Hindlimb End-Point Force Produced by Intraspinal Electrical Stimulation of the Cord

Michel A. Lemay, *Member, IEEE*, James E. Galagan, Neville Hogan, and Emilio Bizzi

***Abstract*—The ability to produce various force patterns at the ankle by microstimulation of the gray matter of the spinal cord was investigated in spinalized frogs. We evaluated the recruitment properties of individual spinal sites and found that forces increase linearly with activation level in the low-force range studied, while the structure of the force pattern remains invariant. We also measured the responses produced by coactivation of two spinal sites activated at two pairs of stimulation levels. Responses were measured at the mechanical level by recording forces at the ankle; and, at the muscular level by recording the electromyographic (EMG) activity of 11 hindlimb muscles. We found that for both pairs of activation, the forces under coactivation were the scaled vectorial summation of the individual responses. At the muscular level, rectified and integrated EMGs also summated during coactivation. Numerous force patterns could, thus, be created by the activation of a few individual sites. These results suggest that microstimulation of the circuitry of the spinal cord (higher order neurons than the motoneurons) holds promise as a new functional neuromuscular stimulation (FNS) technique for the restoration of multi-joint movements.**

***Index Terms*—Electromyography (EMG), functional electrical stimulation (FES), interneurons, spinal cord stimulation.**

I. Introduction

FUNCTIONAL neuromuscular stimulation (FNS) of the paralyzed musculoskeletal system has been used in spinal cord injury to restore function to the upper and lower extremities [1]–[5]. However, difficulties arise when a multijoint system with redundant kinematics and multi-articular muscles must be controlled such as for the restoration of gait or in reaching movements. Although various problems have plagued the design of clinical walking systems (see [6] for a review), recruitment and coordination of the muscles necessary to produce an efficient and well-behaved gait pattern have been two of the most significant. Control of end-point behavior via activation of individual muscles is possible, but the complexity of the hardware and software necessary to perform the task increases significantly. Some scheme must be devised to coordinate the action of the controllers around each joint [7].

Various research groups have shown that the spinal cord is highly organized [8]–[12] and is involved in the coordination of the various muscles necessary for multijoint movements. Studies in various lower vertebrates and mammals have shown the existence of central pattern generators (CPGs) for gait; spinal networks of neurons whose organization can produce rhythmic timed activation of the muscles involved in swimming or gait [13]–[15]. Training programs with spinal cord injured individuals have shown that (through treadmill exercises) the walking pattern of humans can be improved, suggesting that CPGs exist in humans [16], [17].

Giszter and colleagues in frogs [18], Tresch and Bizzi in rats [19], and Lemay and Grill in cats [20] have shown that electrically activating regions of the spinal cord occupied by higher order neurons produces a coordinated convergent pattern of forces at the limb's end point. These fields are of a few distinct types, but have been shown to sum vectorially (in frogs and rats) producing intermediate fields [19], [21]. In this paper, we demonstrate that the field's strength can be modulated by the parameters of excitation, but that the structure of the fields remain essentially the same. We also show that vector summation holds up when each field's strength is modulated by varying the stimulation level. These results suggest a particularly simple mechanism by which the motor control system could produce a rich variety of behaviors from a limited number of movement primitives. The results also suggest that electrical stimulation can be used to produce the same rich variety of behaviors—using a limited number of electrodes activating a few selected regions of the paralyzed spinal cord in a graded manner.

The frog preparation was used in this research. The evidence to date suggests that field properties are similar in the frog and higher vertebrates (rats [19], cats [20]). The simpler preparation allows a greater number of studies to be conducted to evaluate

Manuscript received April 11, 2000; revised October 4, 2000. This work was supported by the Paralyzed Veterans of America Spinal Cord Research Foundation SCRF Grant 1602 and NIH Grants NS09343 and AR40029.

M. A. Lemay was with the Department of Mechanical Engineering, Massachusetts Institute of Technology, Cambridge, MA 02139 USA. He is now with the Department of Neurobiology and Anatomy, MCP Hahnemann University, Philadelphia, PA 19129 USA.

J. E. Galagan was with the Department of Brain and Cognitive Sciences, Massachusetts Institute of Technology, Cambridge, MA 02139 USA. He is now with the Whitehead/Massachusetts Institute of Technology, Institute for Genome Research, Cambridge, MA 02139 USA.

N. Hogan is with the Departments of Mechanical Engineering and Brain and Cognitive Sciences, Massachusetts Institute of Technology, Cambridge, MA 02139 USA.

E. Bizzi is with the Department of Brain and Cognitive Sciences, Massachusetts Institute of Technology, Cambridge, MA 02139 USA.

Publisher Item Identifier S 1534-4320(01)01779-X.

the functional potential of the technique as a substitute to the damaged neural system. The evidence gathered in this animal can also be used to guide the design of experiments in more complex but less robust animal preparations.

II. Methods

A. Surgical and Field Reconstruction Technique

Bullfrogs (*rana catesbiana*) were spinalized by transecting the cord at the level of the *calamus scriptorius*. The lumbar area was exposed by removing the spinal arches of the fourth, fifth, and sixth vertebrae. Motor responses were elicited by microstimulating the spinal cord in what we estimated to be the lateral and intermediate neuropil zones. Cord penetrations were made 150–500 μm from the midline at depths of 400–1200 μm. Depth was measured from the number of microdrive turns from the point of electrode entry visualized with a microscope. The validity of the stereotaxic coordinates were verified in a number of animals by marking electrode locations with electrolytic lesions (10 μA, 15 s), and visualizing them in a post-mortem histology analysis (details in [18]). In the animals tested, the lesions were located in the lateral and intermediate neuropil zones of the spinal cord gray matter (see Fig. 1). The stimulus consisted of a train of cathodic current impulses delivered via a high-impedance stainless steel electrode [impedance: 1–10 MΩ, tip diameter: 0.5–1 μm (no insulation), manufacturer: Frederick Haer & Co., ME]. The mechanical forces at the ankle were measured using a six-axis force transducer (ATI 310) sampled at 50 Hz. We limited our analysis to the x–y plane, which corresponded approximately to the horizontal plane, i.e., the plane of motion during swimming behavior [see Fig. 1(a)]. Fields representing the force vector orientations throughout the workspace were constructed by measuring forces at several different spatial locations [as in Fig. 1(b)], constructing a tessellation of the points, and interpolating each vector within a triangle by a linear interpolation based on the three measured corner vectors. The forces at each of the triangle's corners yielded one force vector ($\mathbf{F_x}$, $\mathbf{F_y}$), as well as one position (x, y) coordinate. Combining the three corners of the triangle yielded six unknowns and six equations, i.e.,

$$\begin{aligned}
\mathbf{F}_{x1} &= a_{1,1}x_1 + a_{1,2}y_1 + a_{1,3} \\
\mathbf{F}_{y1} &= a_{2,1}x_1 + a_{2,2}y_1 + a_{2,3} \\
\mathbf{F}_{x2} &= a_{1,1}x_2 + a_{1,2}y_2 + a_{1,3} \\
\mathbf{F}_{y2} &= a_{2,1}x_2 + a_{2,2}y_2 + a_{2,3} \\
\mathbf{F}_{x3} &= a_{1,1}x_3 + a_{1,2}y_3 + a_{1,3} \\
\mathbf{F}_{y3} &= a_{2,1}x_3 + a_{2,2}y_3 + a_{2,3}. \qquad (1)
\end{aligned}$$

The six parameters, $a_{i,j}$, were calculated by equating the forces measured at the corners of the triangles to the $\mathbf{F}_{xi}$, $\mathbf{F}_{yi}$ given by the previous equations, with x_i and y_i equal to the spatial locations of the triangle's corners. Forces within a triangle were estimated by using the $a_{i,j}$ parameters associated with that triangle, as in Fig. 1(d). We constructed our triangulation to minimize the distance between the interpolated point and the triangles' vertices. We routinely verified the appropriateness of our spatial sampling density by dividing the workspace into a different set of triangles and comparing the field obtained with this different triangulation to the one obtained with the original. Differences found were minimal: typically less than 10% of the vectors differed by more than 10°, with a maximum deviation of 20° in the worst case.

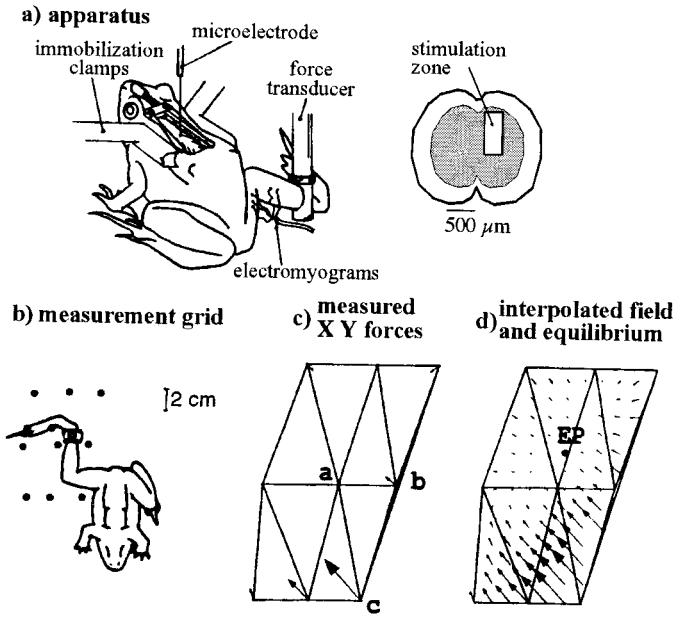

Fig. 1. Experimental setup and field measurement technique. (a) Schematic of the hardware and animal setup as well as the region of electrode penetrations. The frog is held horizontally by side clamps and a pelvic clamp (not shown). The ankle is attached to a movable six-axis force transducer, and EMGs are recorded via intramuscular electrodes. Forces are evoked by microstimulating the spinal gray via a microelectrode inserted dorsally. The graphic on the right illustrates the lateral and intermediate neuropil zones of the gray matter where electrodes were inserted. (b) Relationship between the hindlimb workspace and the locations at which the forces evoked are measured. (c) Forces in the horizontal plane (X–Y) measured at the locations shown in (b) and the division of the area into triangles. (d) Interpolated field—forces within a triangle are obtained by a linear interpolation based on the three corner vectors to give a representation of the force orientation and magnitude throughout the workspace (see text for details) (adapted from [18]).

The two-dimensional interpolation procedure is a simple extension of the univariate interpolation of one-dimensional data. In univariate interpolation the data points are joined by straight-line segments and the value between points is given by the equation of the line joining the two points. In our case, the forces within a triangle are interpolated from the forces measured at the vertices. The interpolating functions are continuous since neighboring triangles share two vertices, but not smooth since the $a_{i,j}$ parameters may change abruptly from one triangle to the next (similar to the line segments for the univariate case).

B. Recruitment Properties of Single Spinal Site Stimulation

We investigated the effects of four stimulation parameters: pulse amplitude (PA); pulse duration (PD); stimulation frequency (SF); and, train duration (TD) on: 1) force magnitude, and 2) field structure. One of the activation parameters was varied between just subthreshold values, to values producing approximately 1–2 N, which we estimated to be about 20% of maximal force (based on jumping experiments [22]), while the other parameters were kept at constant values known to produce

respectable responses. Higher forces could be produced but tended to cause motion of the cord and were typically avoided to prevent electrode movement. Only one parameter was varied for a particular stimulation site. PA was varied between 0.5 and 7 μA, TD was varied between 100–500 ms, PD between 100–600 μs, and SF between 5–80 Hz. The pulse amplitude range was chosen to limit the diameter of the direct stimulation sphere to less than 100 μm [23], [24], although the actual volume stimulated might have been larger due to the activation of neural fibers. On one occasion, we were able to further increase the stimulation without causing cord motion (field ff4 of Fig. 3).

We analyzed the effects of these four stimulation parameters on the time history of the forces; and, on the equilibrium position and structure of the active fields, i.e., the fields reconstructed from the total recorded force minus the passive force. The structure of the fields were analyzed both for change in force vector orientation and change in the vectors' relative magnitudes, i.e., whether the largest vector in a field at one stimulation level was at the same position for the same stimulation site activated at a different stimulation level. Details of the analysis are presented in the next section.

These experiments were carried out on five frogs at 17 stimulation sites. Effects of SF were studied at five sites, and those of PA, PD and TD at four sites each.

C. Dual Sites Activated at Two Different Levels of Stimulation

We investigated the modulated summation of two sites producing fields of different kinds to verify whether linear vector summation (shown by [21]) held up at different activation levels—thereby, allowing us to produce multiple force patterns with a few basic types. While Mussa-Ivaldi and his colleagues showed that a third type could be produced with two sites, we wanted to demonstrate that you could produce four fields with two by modulating the activation to each site. In order to do this, two sites producing different patterns of forces were found and the individual responses of each site to two levels of stimulation were measured. The two sites were then costimulated with one site being activated at the higher stimulation level and the second at the lower stimulation level. The levels of activation given to each site were then switched and a second costimulation measurement was taken. Fields were reconstructed by measuring the force responses throughout the workspace as described above.

These experiments were conducted on nine frogs over 11 experiments at 22 stimulation sites. During one experiment, we used only one high–low combination of stimulation parameters, therefore, we have results for 21 combinations of stimulation parameters.

To investigate the nature of force field costimulation at the level of muscle activation, we measured EMG activity in 11 hindlimb muscles (*rectus internus, adductor magnus, semimembranosus, semitendinosus, iliopsoas, vastus internus, rectus anternus, gastrocnemius, biceps femoris, sartorius, vastus externus*) in eight of the above experiments and in one additional experiment where a single stimulation combination was used and the two fields were of the flexion withdrawal type—for a total of 16 combinations of stimuli parameters. EMGs were measured using Teflon coated stainless steel bipolar electrodes (A-M Systems Inc. cat no. 7935) implanted in the muscles of interest. Implantation was performed by: 1) opening the skin; 2) separating the muscles gently by blunt dissection (except for the deep ones where the electrodes were implanted by palpating the muscles and location was verified post-experimentally); and 3) threading the electrodes directly into the muscles. Raw EMGs were amplified, sampled at 1000 Hz, rectified, and integrated.

III. Data Analysis

A. Linear System Definition

For a system to be linear it must be closed under addition and scalar multiplication

$$L(c_1u_1 + c_2u_2) = c_1L(u_1) + c_2L(u_2) \tag{2}$$

where $L(u)$ is the output of the system to an input u and c is a scalar constant. In order for the interneuronal circuitry to be linear, we must show that the field's response modulates linearly with stimulus strength [$L(cu_1) = cL(u_1)$] and that vector summation holds under modulation of the individual field's strength [see (2)]. The experiments described in Section II-B evaluate the scalar multiplication condition but say nothing about the addition condition, while the Section II-C experiments evaluate the addition and multiplication conditions for two inputs at two levels.

B. Single-Site Recruitment Curve

The recruitment properties of the stimuli effects during single-site stimulation were quantified by studying the relationship between the active force magnitude at each position in the workspace and the charge, which is the measure of the amount of electrical stimulation delivered to the tissue (in units of coulombs). This relationship is the muscle force recruitment curve. In traditional FNS (nerve or muscle) this relationship exhibits a low–slope region, followed by a linear region as stimulation increases and, finally, a plateau when saturation is reached [25], [26]. In this study, the peak–force magnitudes at each position were normalized to the maximum force at that position and polled together to give one curve of normalized force vector magnitude as a function of charge. Since we did not reach saturation and our initial low-slope region was restrained, the relationship could be fitted to a linear model and that fit was evaluated using the standard correlation coefficient r.

C. Field Structure Comparison

Fields' structures were compared for both angular and magnitude deviations. Sets of force vector angles: ϕ_i and φ_i, measured throughout the workspace for different stimulation levels, (single site) and/or for different sites (dual sites), were compared by constructing the differences $\Delta\theta_i = \phi_i - \varphi_i$; and, computing the mean angle and angular deviation [27] to obtain a measure of the similarities in the angular directions of the vectors measured at different activations, but at the same spatial location. To compare for possible differences in the relative magnitude

of fields at different stimulation levels, we measured the ratios of normalized force vector magnitude at the sample locations in the workspace. Normalization was to the maximum force vector measured in the workspace at that activation level and differences in relative magnitude indicate that forces are not of the same magnitude at the same location once the field's maximum force level is accounted for. For the costimulation experiments we did not normalize the vectors since, in that case, we were interested in comparing actual magnitudes between the costimulation response and the sum of the individual responses. Ideally, this ratio should be 1.0 since the force vector of the normalized/nonnormalized fields should be identical if the fields present the same relative magnitude. We limited our analysis to vectors whose force magnitude was at least 0.1 N to avoid comparing force vectors with signal to noise ratios less than four.

D. Summation Hypothesis during Costimulation of Individual Sites Activated at Two Different Levels of Stimulation

Using the above measures to compare fields, we evaluated the hypothesis that the field obtained via costimulation was a scaled linear summation of the individual responses obtained, i.e.

$$\mathbf{F}_{\mathrm{A\,low\,B\,high}} = s[\mathbf{F}_{\mathrm{A\,low}} + \mathbf{F}_{\mathrm{B\,high}}]$$

and

$$\mathbf{F}_{\mathrm{A\,high\,B\,low}} = s[\mathbf{F}_{\mathrm{A\,high}} + \mathbf{F}_{\mathrm{B\,low}}] \tag{3}$$

where

- $\mathbf{F}_{\mathrm{A\,low}}$ and $\mathbf{F}_{\mathrm{A\,high}}$ represent the fields obtained with lower and higher level of stimulation for site A;
- $\mathbf{F}_{\mathrm{B\,low}}$ and $\mathbf{F}_{\mathrm{B\,high}}$ represent the same for site B;
- $F_{\mathrm{A\,low\,B\,high}}$ represents the field obtained via costimulation of site A with the higher stimulation level and site B with the lower level and vice versa for $\mathbf{F}_{\mathrm{A\,high\,B\,low}}$.

s is obtained via least squares and for a linear system is required to be equal to one. Mussa-Ivaldi and collaborators have shown that the fields sum up vectorially for two sites stimulated at one activation level [21]. Our aim was to see if the summation could be modulated by varying the activation of each individual site. We limited ourselves to two stimulation level combinations to minimize fatigue, and chose high–low combinations in order to maximize the angular differences between summated responses. Since our hypothesis called for linear gradation of the force magnitude with stimulation amplitude (with no change in the force direction), we were concerned that a low–low and high–high combination would produce summed vectors with similar orientations for both costimulation responses. We evaluated the fields at the time of maximum amplitude (i.e., the time of peak force amplitude) but, in a few instances, we verified the summation throughout the force response time course and found that the scaling coefficient did not vary significantly through time.

E. EMGs during Costimulation Experiments

Using a theoretical analysis, Galagan and colleagues [28] predicted that if vector summation holds during costimulation of two sites, then the isometric force produced by a muscle during costimulation must be the sum of the isometric forces produced during stimulation of each site individually. Under the assumption that isometric force is linearly related to the muscle's rectified and integrated EMG activity (a valid assumption under isometric condition and low force levels [29], [30]), this predicts that the rectified integrated EMGs under costimulation should be the sum of the rectified integrated EMGs during the individual responses.

The EMGs for each muscle in each trial were rectified and integrated, and the rectified integrated EMGs during the individual stimulation trials were then summed and plotted against the rectified integrated EMGs during costimulation. To minimize the effects of crosstalk, only muscles where the EMGs were above a threshold were analyzed. This threshold was 10% of the peak of the largest sampled EMG among all the muscle EMGs in a given trio of individual and costimulation responses. The value of 10% was determined experimentally by implanting two neighboring muscles with EMG electrodes, denervating one and comparing the EMG response to cutaneous stimulation of the intact muscle to the one in the denervated muscle. We found that the crosstalk was less than 10% of the peak EMG in the intact muscle.

IV. Results

A. Single-Site Recruitment Modulation

Active force magnitude was modulated by all four parameters as shown in Fig. 2, which shows the time course of force magnitude for one position in four different fields/activation sites, with one of the four activation parameters being varied. The figure also shows that the time course of the forces can be of different types. Some force responses die away almost immediately, e.g., responses with PA modulation, while others present either a pulse and plateau type of response, e.g., $\mathrm{PD} = 600\ \mu$s, or a pure plateau response; for example, $\mathrm{PD} = 300\ \mu$s. The plateaus extend beyond the 1 s of data collection, and typically last for 2–3 s. Such plateaus are not encountered during motoneuron or nerve activation [31], [32], and as such are an indication of a sustained neuronal network firing.

The average (over all sampled positions) normalized (to maximum force at that spatial location) force magnitude *versus* charge is shown in Fig. 3 for all 17 fields. The average correlation coefficient of the curves at all locations to a linear fit was >0.9 in 16 of the 17 sites. The one exception was ff4, where the SF was increased to a level which caused an uncharacteristic change in the orientation of the forces. For the range of forces ($0.1 - \approx 3$ N) and stimulation parameters studied (see Sections II), we conclude that force recruitment via microstimulation of the gray matter interneurons is linear. The time course of force production may vary from site to site, with some sites presenting an extended response, while others terminate rapidly. The orientation of the active force vector was constant throughout each stimulating trial as already demonstrated in [18].

B. Field Structure when Modulating the Activation of a Single Site

Fields at different stimulation levels were compared by computing the $\Delta\theta_i$ and the ratios of normalized force vector mag-

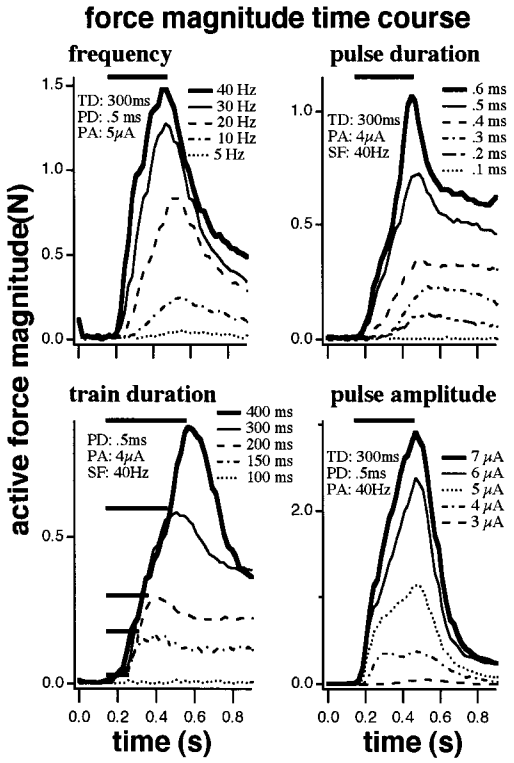

Fig. 2. Time course of the active force magnitude at one location in the workspace and the effects of the four stimulation parameters for four different stimulation sites. The bars indicate the time stimulation was on and the responses are from single trials. As seen by [18], the time course of the response was of three types: pulse—a rapid on/off behavior (e.g., pulse amplitude), a pulse and plateau, a peak in force followed by a long lasting (2–3 s) plateau (e.g., 0.6 ms pulse duration), and a plateau (e.g., 0.4 ms pulse duration).

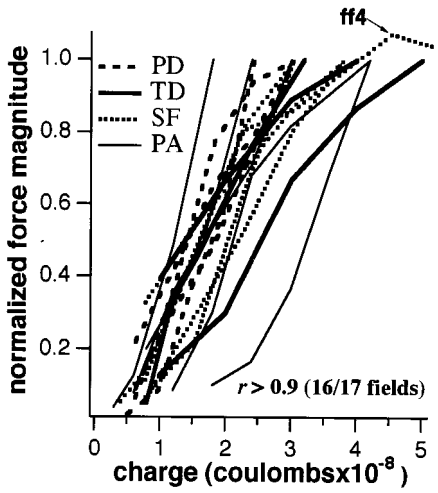

Fig. 3. Average normalized force magnitude (over sampled locations) *versus* injected charge for 17 spinal sites. The coefficient of correlation is >0.9 in all cases but ff4, a site where the stimulation was increased past 4.5×10^{-8} coulombs, causing the field structure to change. The only significant difference between the average slopes of the lines for the four parameters of stimulation (PD, PA, TD or SF) was between PD and PA (Fisher's PLSD, P-value $= 0.004$).

nitudes (described in Section II) at the sampled locations. The entire population of difference angles and magnitude ratios are presented in Fig. 4(a) and (b), respectively (excluding the stimulation levels that caused apparent changes in the field structure of ff4). These populations are the difference angles and magnitude ratios obtained when comparing fields at each sampled position for different activation levels (see Section III-B). The mean angular difference was 1.3° and the angular deviation (the equivalent of the standard deviation in linear statistics) was 11.8°. A χ^2 goodness-of-fit test revealed that the angular difference population fitted a von Mises distribution (the circular statistics equivalent of the normal distribution, see [27] for further information on circular statistics) with a mean angle of 1.3°, and a parameter of concentration $\kappa = 23.9$. For a sample size of nine (the typical number of positions measured), the mean angular difference and 95% confidence interval were $1.3° \pm 7°$ (95% CI). To summarize, less than 10% of the angular differences between vectors obtained at the same spatial location but at different activation levels were greater than 20° and almost 80% were within 10°. Vectors maintained the same orientation with activation modulation.

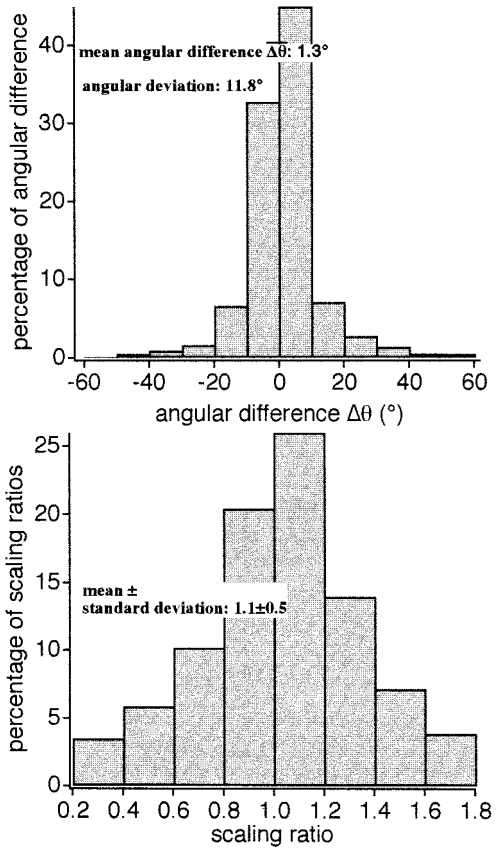

Fig. 4. (a) Distribution of the angular differences between vectors measured at the same position but at different levels of activation for each of the 17 stimulation sites. Almost 80% of the differences are between $-10°$ to $+10°$, mean angle is 1.3°, and the angular deviation (the equivalent of the standard deviation in linear statistics) is 11.8°. (b) Distribution of the magnitude ratio between vectors measured at the same position but at different levels of activation for each of the 17 stimulation sites. The mean magnitude ratio is 1.1 with a standard deviation of 0.5.

The mean magnitude ratio was 1.1 with a standard deviation of 0.5. χ^2 goodness-of-fit tests revealed that the ratios of normalized force vector magnitudes fitted a normal distribution. Using the standard deviation of this sample as our estimate of the population variance ($n = 1039$, a large sample), we calculate that the 95% confidence interval for the magnitude ratio is 1.1 ± 0.1 (95% CI with sample size of nine), which includes 1.0,

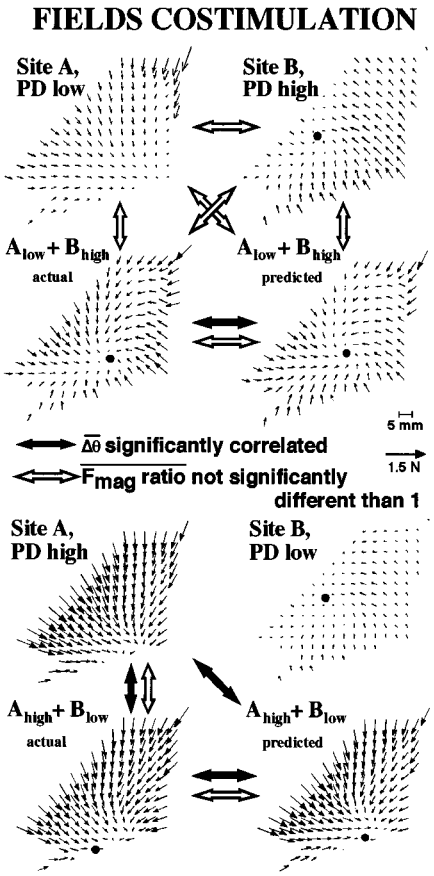

Fig. 5. Vector summation of force vectors when costimulating sites at different activation levels. The top panel shows the individual fields obtained when site A was stimulated at the lower PD and site B at the higher one, and the actual (site A and B activated simultaneously) and predicted (from linear summation) fields obtained from costimulation of the two sites. The bottom panel shows the results when the levels of activation were switched. Similarity between fields is indicated by a black arrow indicating no difference in average angular deviation across the measured vectors (no evidence of directness based on Rayleigh test [27], statistical significance $\alpha = 0.01$), and a white arrow indicating that the force magnitude ratio across positions is not different than 1 (t-test, $\alpha = 0.05$). Note that in the top panel, the actual and predicted fields were similar to each other, but dissimilar to the other fields. In the bottom panel, the actual and predicted fields were similar but the actual field was also similar to site A alone since the forces produced by site B are low. The fields produced by the two combinations of activation levels (top and bottom panel) were different from each other, showing the possibility of creating a variety of fields by modulating the contribution of each original site to the summated response.

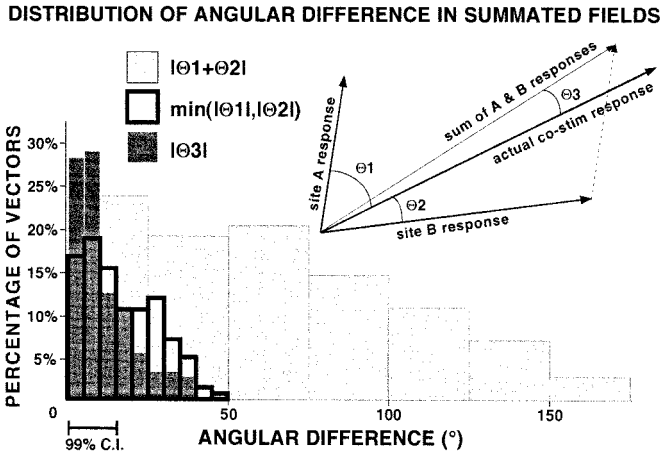

Fig. 6. Histogram of the distribution of the absolute angular differences for the experiments exemplified in Fig. 5. Absolute angular differences shown are between (a) two individual fields (in light gray, n: 264); (b) the actual costimulation response and the closest individual response (thick line, n: 143); and (c) the scaled vector sum of the individual responses and the actual costimulation response (in dark gray, n: 183). The height of each bar represents the percentage of vectors whose angular difference (for the vectors shown in the upper right graph) falls within the range the bar occupies on the abscissa. The 99% CI was calculated based on a sample size of nine (the typical number of positions at which a field was measured) extracted from the population represented in Fig. 4(a). Approximately 70% of the angular differences between actual and sum (Θ_3) fall within that interval, while 50% of the angular differences between the actual costimulation response and the closest individual response ($\min(|\Theta_1|, |\Theta_2|)$ do. Those populations' mean angles are not statistically different from zero, but Θ_3 is more significantly concentrated near zero.

the necessary ratio if we are to conclude that activation affects the magnitude but not the structure of the fields.

Only three of the 17 (18%) stimulation sites showed an equilibrium position in the active fields, and the equilibrium position did not vary with the activation level. Two of the sites showed a single equilibrium point that over three or four stimulation levels stayed within a 3 and 7 mm diameter, respectively. The third field had two equilibrium points that were 22 mm apart with a region of low forces (<0.05 N) between the two. These results are further evidence that the structure of the field remains unchanged with variation in the activation level.

C. Summation During Costimulation of Individual Sites Activated at Two Different Levels of Stimulation

As mentioned above, costimulation was evaluated in 11 experiments over nine frogs, given a total of 21 costimulation combinations. Fig. 5 presents an example of linear summation of the force vectors and of modulation of the sum by varying the stimulation parameters of each individual site. As can be seen from the graph, the predicted and actual sums are very close to each other yet different from the individual fields for the top combination of activation levels. The statistical analysis used was a Rayleigh test (at $\alpha = 0.01$), which tests for the significance of directness, i.e., whether the data are concentrated around a point, in this case 0°. Since the test is not very powerful we made the decision to use a 99% confidence level before rejecting the hypothesis of randomness. For the bottom combination of activation levels the results are similar. In that case the response at site A is much larger than at site B, and the actual costimulation response is similar to site A's response (minus the equilibrium point) in addition to being similar to the predicted sum. Nevertheless, the figure shows that by modulating the activation of each site, it was possible to create two costimulation responses that were different ($\Delta\theta = 2.3° \pm 54°$, P-value $= 0.04$), but similar to the linear summation of the two individuals responses.

Fig. 6 presents the distribution of the absolute values of the angular differences for all the summed fields evaluated. The angular differences between two force vectors at each of the positions in the workspace for each of the summation experiments is depicted on the figure. The figure includes distributions for the differences between the individual sites' responses, between the actual costimulation response and the closest individual response, and between the actual costimulation response and the sum of the individual responses. The 15° 99% confidence interval shown in Fig. 6 was constructed using the distribution of

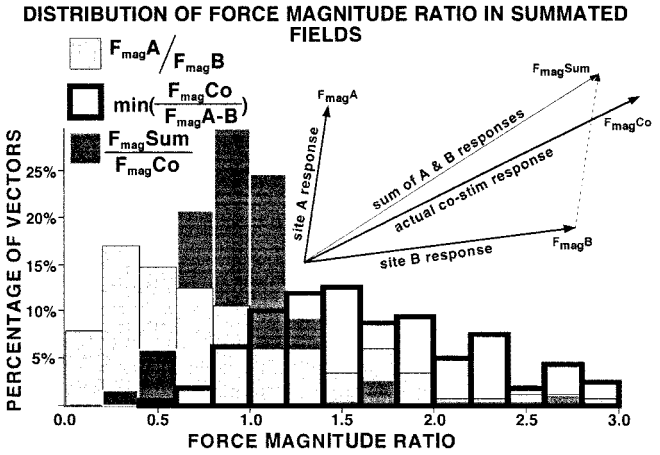

Fig. 7. Histogram of the distribution of the force vectors magnitude ratios for the experiments exemplified in Fig. 5. Magnitude ratios shown are between (a) two individuals fields (in light gray); (b) the actual costimulation response and the closest individual response (thick line); and (c) the scaled vector sum of the individual responses and the actual costimulation response (in dark gray). In this case, the height of each bar represents the percentage of vectors whose force magnitude ratio falls within the range the bar occupies on the abscissa. The distribution of the magnitude ratio between costimulation and summated responses (F_{mag}Sum/F_{mag}Co) presents the highest proportion of ratios in the 0.8–1.2 range: 54%. That proportion drops to 16% for the magnitude ratio between the individuals fields (F_{mag}A/F_{mag}B), and the minimum ratio between the costimulation response and the individual responses ($\min$(F_{mag}Co/F_{mag}A-B).

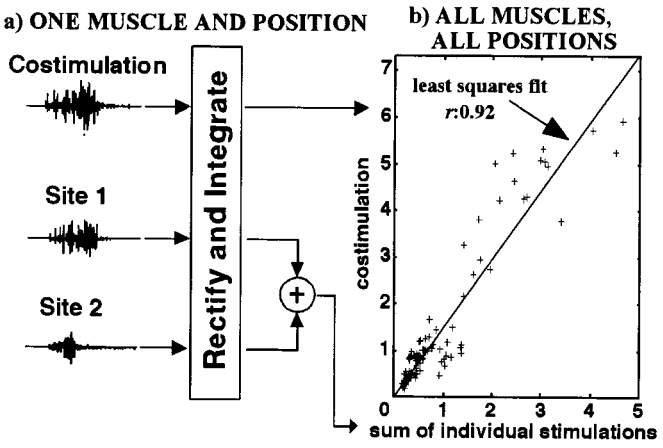

Fig. 8. Analysis of the relationship between actual EMGs of 11 hindlimb muscles during costimulation *versus* the sum of the EMGs during stimulation of the individual spinal sites. EMGs of each muscle at each position were rectified and integrated over time. The rectified and integrated EMGs produced by activation of the individual spinal sites (for each muscle at each position) were then summated and compared with the rectified integrated EMGs (of each muscle at each position) produced during costimulation of the spinal sites (a). An example of the correlation between the sum of individual stimulation EMGs and the actual costimulation EMGs for one trio of single and costimulation responses is given in b, for all muscles studied at each position measured. The correlation coefficient for that particular combination of stimuli was 0.9. The average correlation coefficient for the 16 costimulation stimuli pairs studied was 0.87 ± 0.07. We conclude that linear summation of force output is achieved via summation of the individual drives to the muscular system.

the angular differences between fields at different stimulation levels (Fig. 4) as the parent population, and calculating the interval based on a sample size of nine (number of spatial positions to construct a field) with a mean of zero. Approximately 70% of the angular differences between actual and sum (Θ_3, Fig. 6) fall within that interval, while 50% of the angular differences between the actual costimulation response and the closest individual response [$\min(|\Theta_1|, |\Theta_2|)$, Fig. 6] do so. Mathematically, the mean angles of both populations of vectors are not statistically different from zero, but Θ_3 is more significantly concentrated near zero. Angular deviation for Θ_3 is 15°, while it is 25° for $\min(|\Theta_1|, |\Theta_2|)$.

Fig. 7 gives the magnitude counterpart of Fig. 6. The distribution of the magnitude ratio between costimulation and summated responses presents the highest proportion of ratios in the 0.8–1.2 range: 54%. That proportion drops to 16% for the magnitude ratio between the individual fields, and the minimum ratio between the costimulation response and the individual responses. The distribution of the magnitude ratio between costimulation and summated responses is also the only one whose mean and median are within 0.1 of 1.0, the expected ratio under summation.

The scaling coefficients s [of (3)] average and standard deviation are 1.2 ± 0.2. Although this average is strictly speaking different than 1.0 (P-value $= 0.0003$, student t-test), it is no different than Mussa-Ivaldi *et al.*'s average in their original study: 1.1 ± 0.4 (larger standard deviation) [21]. Based on these factors, we conclude that summation respects strict linearity.

To verify the validity of the scaled vectorial summation hypothesis we also evaluated a weighted sum model, i.e.

$$\mathbf{F}_{\mathrm{A\,low\,B\,high}} = s_1\mathbf{F}_{\mathrm{A\,low}} + s_2\mathbf{F}_{\mathrm{B\,high}}s$$

and

$$\mathbf{F}_{\mathrm{A\,high\,B\,low}} = s_1\mathbf{F}_{\mathrm{A\,high}} + s_2\mathbf{F}_{\mathrm{B\,low}}. \tag{4}$$

We found that the residuals (distance between the actual and fitted costimulation responses) were no better than for the scaled vectorial summation. We also evaluated a winner-take-all hypothesis (i.e., costimulation response fitted to a scaled version of the best fitting single site response) and found that the residuals were higher than for the vectorial summation or weighted summation models. Simple linear addition of the individual sites' force vectors is, therefore, an adequate representation of the force output during costimulation of individual sites.

The average difference between the two scaling coefficients for a pair of costimulation levels is 0.052 ± 0.238 standard deviation (SD) . This difference is not significantly different from zero (P-value $= 0.49$, paired t-test), indicating that the same scaling coefficient holds for the two pairs of activation levels.

D. EMGs During Costimulation Experiments

The correlation coefficients of a linear least square fit of summated to actual integrated EMGs for all muscles at all positions in the workspace for the 16 costimulation stimuli pairs were calculated as demonstrated in Fig. 8. The average correlation coefficient is 0.87 ± 0.07, indicating that Galagan *et al.*'s prediction holds true [28]. Summation of force output is achieved via summation of the individual drives to the muscles. These results imply that numerous muscles will be coactivated during movements composed using coactivation of spinal sites. The coactivation may lead to rapid muscle fatigue, although the recruitment order of the muscle fibers activated by the stimulated spinal sites is unknown at this time. Muscle fibers may be recruited in a physiological manner (slow fatigue resistant fibers

first, followed by the faster less fatigue resistant ones) by the intraspinal microstimulation, which would delay the onset of muscular fatigue.

E. Summary

Results in Sections IV-A and -B demonstrate that the system in the force range studied is linear under multiplication. Multiplication of the stimulation parameter results in a multiplication of the field output. Force increases linearly with stimulation, but the field structure is maintained. Reference [18] already demonstrated force increase with higher stimulation level, but the quantitative nature of the relationship was not studied. Results Section IV-C shows that the system is also linear under addition. The force vectors summate vectorially. In summary, force magnitude can be graded continuously and vectorial summation holds with no change in the scaling coefficient when the activation is modulated. These two results combined indicate that a continuum of fields can be produced by coactivation of a few selected sites at varying levels of activation. By demonstrating that summation is maintained over varying levels of activation we are expanding the results of [21] and demonstrating that the fields' sum may be modulated by varying the individual field's activation level. Furthermore, we demonstrated that the mechanism responsible for the phenomenon is simple summation of the individual muscle drives.

V. Discussion

A. Motoneurons Versus Interneurons

Current clinical FNS systems are based on stimulation of the last-order neurons, i.e., the motoneurons, although it has been known since Sherrington [44] that part of the substantial repertoire of movements observed in vertebrates is programmed at the level of the spinal cord, and can thus function after injury to higher portions of the cord. Thus, as expressed more recently by Burke, "One of the major challenges facing clinical neurobiologists is how to exploit the untapped reserves of coordinated movement contained in the spinal cord circuits of patients with a functionally isolated spinal cord [45]." The work presented here investigated the recruitment properties of the end-point force patterns elicited by stimulating interneuronal regions in the gray matter of the frog spinal cord. Locating the electrode into interneuronal regions does not guarantee that only the interneurons are activated since axons of distally located cells, or motoneurons dendrites (which, in the frog, extend into the dorsal regions [46]) may be electrically activated. Although, the specificity of the neuronal structure activated by microstimulation is low, a number of studies indicate that interneurons are indeed activated by the stimulation and that the organization is not produced by motoneurons pools organization or afferent reflexes.

In the original study describing this spinal organization, Giszter and collaborators [18] used sulforhodamine (a dye) to demonstrate that the spread of motoneuron activation during expression of a force pattern was two orders of magnitude larger than what would be expected from direct activation of motoneurons by the electrode. An even more convincing observation is the work of Saltiel and colleagues [42] who repeated similar intraspinal stimulation experiments but used focal iontophoresis to deliver microvolumes (spread estimated at 150–270 μm radius) of N-methyl-D-Aspartate (NMDA, a compound know to activate only somas and dendrites) into the same spinal cord regions of spinalized frogs. Similar force patterns were found for the chemical microstimulation as the ones produced by electrical microstimulation. To distinguish between interneurons and dendrites of motoneurons as the two possible elements activated by NMDA, tetrodotoxin (TTX) was applied focally at sites responding to NMDA. TTX is a pharmacological agent that blocks cell spiking, but still allows dendrite activation. If the force patterns were mediated by interneuronal activation, TTX application should abolish the response evoked by NMDA, but if the fields are the results of motoneurons' dendrite activation the TTX should not have such an effect. Results demonstrated that application of TTX abolished the forces produced by NMDA and that washing out the TTX with a bolus of saline returned the responsiveness to NMDA delivery. The NMDA results are a strong indication that the force patterns are not due to activation of remote cells' axons, or motoneurons' dendrites activation. Further evidence against a strictly afferent reflex mechanism is provided by the fact that the same force pattern can be elicited by stimulating the same spinal region in chronically deafferented animals (both in the frogs [18], [47] and rats [19]). The results of the aforementioned controls strongly support the hypothesis that the force patterns are due to the activation of interneurons.

Selective intraspinal electrical activation of motoneuron pools has been demonstrated ([33], [34], [48]) and is a possible alternative to interneuronal stimulation, although, the added benefits of the coordination provided by the spinal circuitry would be lost with this method. A greater selectivity in muscle activation would be expected, a selectivity similar to the one provided by intramuscular electrodes of nerve cuffs on individual nerve branches. The benefits of this approach over muscle or nerve stimulation are that: 1) electrode breakage is possibly reduced since electrodes would be implanted in an area subjected to far less strain and movement than nerves or muscles and 2) the regions containing the motoneurons is fairly small which should allow the activation of every hindlimb muscle with electrodes implanted in a small region.

B. Linearity and Nonlinearity

This paper presents evidence in support of a linear model of end-point force recruitment with intraspinal microstimulation delivered into dorsal interneuronal regions. Two linear processes were demonstrated: linearity of recruitment, and linear summation of force superposition during costimulation. These will be discussed separately.

The first linear relationship is between the end-point force and the stimulation level delivered intraspinally. In clinical FNS applications, stimulation is for the most part delivered intramuscularly, or via nerve activation. The relationship between force and stimulation level is typically sigmoidal in shape, showing a sub-threshold region where no force is produced although charge is being delivered; followed by a region of linear increase

in force with stimulation, then a plateau as the muscle force output saturates despite the increase in stimulation level. This relationship is typical of the muscle studied in isolation, i.e., detached from the surrounding tissue. When the muscle is studied *in situ* (within the limb), spillover to other muscles may occur. This leads to a decrease in force output with increasing stimulation level, the absence of a force plateau, or further increase in force output after a plateau phase—as an agonist muscle is recruited.

We found a linear increase in force output with increases in stimulation for the low-force range studied. In a study of intraspinal microstimulation of the motoneurons pools, Mushahwar and Horch [33] found a similar linear relationship in the low–force range as well as force plateaus at higher force. The presence of a linear relationship, therefore, is not that surprising and the absence of a plateau merely indicates that full muscular recruitment was not achieved. Although the force range studied here appears small when compared to maximal force output, it is within the range used during normal locomotive activities such as swimming [22].The relative (to maximum during jumping) force levels reported here are similar to the relative levels obtained by other investigators using single electrodes implanted in more ventral regions of the cat spinal cord [33], [34]. Tai and colleagues obtained extension torques of about 0.6 Nm [34] (compared with 4.6 Nm produced during jumping [35]), while Mushahwar and Horch [33] reported peak muscle forces of 1.3% to 73% of maximal twitch force obtained by whole nerve stimulation with the majority of the forces generated being in the lower portion of that range. Despite operating in a similar force range, Tai *et al.* [34] found nonlinear recruitment curves between isometric extension torques and stimulation level, while Mushahwar and Horch obtained linear relations for the lower-force range followed by a force plateau for electrodes producing larger forces [33]. While Mushahwar and Horch stimulated exclusively in laminae IX (motoneurons pools), some of Tai *et al.*'s penetrations were more medial into laminae VII and VIII (regions that include the Renshaw cells) which could account for the nonlinear recruitment curves. Our recruitment curves are, therefore, similar to the ones obtained in motoneuron pools, although muscles are coactivated with dorsal stimulation, while single muscles can be activated with motoneuron pool stimulation. Greater forces may be obtainable in both cases by costimulating sites producing similar types of responses, or by increasing the stimulation level applied to an electrode floating relative to the cord. Activation of adjacent neural tissue may occur with the second option as discussed below.

The movement space covered by our measurements fully covers the hindlimb's workspace during swimming and reflex withdrawal and cross-extension reflexes [36], [37]. Movements in the vertical plane are typically not analyzed in motion studies since they are small (see the two cited studies), therefore, our linearity results apply throughout the workspace used during motion and are not subject to the caveats imposed by a limited measurement range as are the force magnitude results.

The most dramatic break in the linearity of the force recruitment we observed (field ff4 of Result Section IV-A) was not related to force magnitude, but to orientation. The change in the structure of the force pattern at higher stimulation was akin to the change in output force measured when spillover of activation to a neighboring muscle occurs. The increase in stimulation level probably activated neighboring neural tissue, thereby, causing the uncharacteristic change in the active force pattern. As with intramuscular electrodes, the electrode location probably plays an important role in determining how much stimulation can be delivered to a site before the activation threshold of neural elements with a different function is reached.

The second linear relationship demonstrated was the summation of the individual responses to stimulation when two spinal sites were coactivated. We demonstrated that the relationship holds when the activation level of two spinal sites is modulated and that the response is mediated by a summation of the muscular activity produced by the individual responses. The force summation principle indicates that a variety of responses can be created by coactivating spinal sites producing different force responses at varying levels of activation. The EMG summation principle indicates that the limits of the phenomenon would occur if muscle activation saturation is reached during costimulation trials. Saturation in any of the muscles would preclude summation of the end-point force responses obtained during the nonsaturating individual responses. Summation would hold even if the recruitment of an individual site was nonlinear, as long as the summation of the muscle drives would not cause saturation in the muscular output.

Prior research has shown that the spinal circuitry exhibits numerous nonlinear phenomena: plateau potentials (i.e., prolonged depolarized states) [38], variation in the stretch-reflex gain as a function of the step cycle [39], and even reversal of reflex gain (from inhibitory to excitatory) depending on the gait cycle phase [40]. The current finding of a linear summation in the force output produced by activation of different spinal sites is, therefore, a somewhat surprising simple outcome. Mussa-Ivaldi and colleagues [21] initially demonstrated the linear summation phenomenon in the frog, followed by Tresch *et al.*'s similar findings in the rat [19]. Our results expand on theirs by demonstrating that the property is preserved when the activation to each site is modulated, giving us the ability to produce force patterns that are a graded combination of the original fields. The initial study also reported a striking nonlinear phenomenon where the response to coactivation of two spinal sites was identical to the stimulation of one of the single sites. The EMG patterns for this phenomenon, termed "winner-take-all," indicated that the muscle activation during costimulation was identical to the muscle activation during the single site stimulation producing the force responses expressed during costimulation of the two sites (Galagan, JE; personal communication).

A number of recent intraspinal microstimulation studies indicate that a number of other phenomena may occur when electrical stimulation is delivered at multiple locations. With a set of four electrodes spaced 0.5 or 1.0 mm apart in the rostrocaudal direction and implanted in the ventral portion of the lumbar enlargement, [41] obtained results where costimulation produced a response that showed either enhancement (up to 500%) or suppression of the knee torque with respect to the individual responses. At one workspace location (as in their study), vectorial summation of end-point force vectors would translate into sum-

mation of single joint torques, while a winner-take-all response would translate into a costimulation torque response equal to the torque obtained for stimulation at one of the electrodes. Both cases are different than the ones obtained in this laboratory, even though the results are expressed in terms of knee joint response instead of end-point response.

Since summation has been observed in a mammal [19], the differences are more likely attributable to differences in electrode location rather than to differences in animal species. Linear summation of end-point force vectors in the mammal was observed for stimulation in laminae I through V, while the results of [41] were obtained for stimulation in what appears to be ventral laminae VII through IX. The inhibition phenomenon may be related to Renshaw cells activation (located mostly in ventral laminae VII [11]), while the enhancement responses might be related to other interneurons being activated (as suggested by [41]). As described in the previous section, the organization reported in the present work as well as in related work [18], [19], [21], [42], [43] is purported to be programmed at the more dorsal interneuronal level. The results obtained for stimulation in more ventral locations seem to support the fact that the linear organization is specific to the more dorsal interneuronal regions, although, the phenomena observed during ventral microstimulation are representative of the cord motor output due to microstimulation.

C. Road to FNS Application

Although frogs are lower vertebrates and have spinal cords with substantial differences from those of mammals [49], results to date indicate that similar force patterns exist in mammals. Force fields have been found in rats and cats, and summation of force vector has been shown in the rat. Thus, it seems that the fields are following the example of the central pattern generator (CPG) of locomotion, which was initially demonstrated in lower vertebrates [15] but was eventually shown to also exist in humans [16], [17], [50]. Since the evidence to date is that spinal organization is maintained with evolution, we hypothesize that recruitment properties similar to the ones presented in this paper are active in the mammalian circuits producing the force patterns described here.

A number of issues still need to be addressed before the technique can be considered for clinical application. The results presented here are limited to isometric observations, while FNS applications are more concerned with motion. A number of research groups are investigating the dynamic behaviors that can be generated with intraspinal microstimulation [51]–[53], and further work is still required. Control issues have only been partially addressed by this paper. The linear gradation of forces and the vectorial summation of forces are beneficial, but not essential. Although we can reproduce some of the control characteristics associated with last-order neuron stimulation, control strategies that utilize the nonlinear properties of the spinal circuitry have yet to be developed. Furthermore, control strategies on how to combine fields to produce the desired end-point trajectory and interactive behavior with the environment must be developed before implantation in humans can be considered (e.g., see [54] for a simulation study showing the benefits of the pulse and plateau types of force response). Although the mechanical property mismatch between the electrode materials used in current clinical applications and the cord typically produce electrode movement and subsequent cord damage [55], Mushawar and Prochazka [53] have successfully implanted multiple single wire electrodes in the cat spinal cord and obtained whole limb movements from stimulation of these electrodes over extended periods of time (over one year). Such progress on both the technical and basic science aspects of intraspinal microstimulation should eventually lead to human applications.

VI. Conclusion

The strength of the force fields produced via electrical activation of spinal interneurons is linearly modulated by the parameters of activation in the range studied (20% of maximal force output), while the orientation and pattern of the forces remain for the most part unaffected. Furthermore, the force levels are in the range of forces used for regular locomotive activities (e.g., swimming), and are sufficient to produce motion. Results also suggest that sites can be coactivated to produce fields that are scaled vector sums of the fields produced by activation of the individual sites and the summation property holds when each site's activation is individually modulated.

References

[1] P. H. Veltink and N. Donaldson, "A perspective on the control of FES-supported standing," *IEEE Trans. Rehab. Eng.*, vol. 6, pp. 109–112, June 1998.

[2] K. L. Kilgore, P. H. Peckham, M. W. Keith, G. B. Thrope, K. S. Wuolle, A. M. Bryden, and R. L. Hart, "An implanted upper-extremity neuroprosthesis. Follow-up of five patients," *J. Bone Joint Surg. Amer.*, vol. 79, pp. 533–541, 1997.

[3] R. Kobetic, R. J. Triolo, and E. B. Marsolais, "Muscle selection and walking performance of multichannel FES systems for ambulation in paraplegia," *IEEE Trans. Rehab. Eng.*, vol. 5, pp. 23–29, Mar. 1997.

[4] R. H. Nathan and A. Ohry, "Upper limb functions regained in quadriplegia: a hybrid computerized neuromuscular stimulation system," *Arch. Phys. Med. Rehab.*, vol. 71, pp. 415–421, 1990.

[5] Y. Handa, T. Handa, M. Ichie, H. Murakami, N. Hoshimiya, S. Ishikawa, and K. Ohkubo, "Functional electrical stimulation (FES) systems for restoration of motor function of paralyzed muscles—Versatile systems and a portable system," *Front Med. Bio. Eng.*, vol. 4, pp. 241–255, 1992.

[6] H. J. Chizeck, R. Kobetic, E. B. Marsolais, J. J. Abbas, I. H. Donner, and E. Simon, "Control of functional neuromuscular stimulation system for standing and locomotion in paraplegics," *Proc. IEEE*, vol. 76, pp. 1155–165, Sept. 1988.

[7] N. Lan, P. E. Crago, and H. J. Chizeck, "Control of end-point forces of a multijoint limb by functional neuromuscular stimulation," *IEEE Trans. Biomed. Eng.*, vol. 38, pp. 953–965, Sept. 1991.

[8] B. Alstermark, H. Kummel, M. J. Pinter, and B. Tantisira, "Integration in descending motor pathways controlling the forelimb in the cat. 17. Axonal projection and termination of C3-C4 propriospinal neurones in the C6-Th1 segments," *Exp. Brain Res.*, vol. 81, pp. 447–461, 1990.

[9] E. Jankowska and S. Edgley, "Interactions between pathways controlling posture and gait at the level of spinal interneurones in the cat," *Prog. Brain Res.*, vol. 97, pp. 161–171, 1993.

[10] A. Lundberg, "Multisensory control of spinal reflex pathways," *Prog. Brain Res.*, vol. 50, pp. 11–28, 1979.

[11] D. A. McCrea, "Spinal cord circuitry and motor reflexes," *Exercise Sport Sci. Rev.*, vol. 14, pp. 105–141, 1986.

[12] S. Rossignol, "Neural control of stereotypic limb movements," in *Handbook of Physiology, Section 12. Exercise: Regulation and Integration of Multiple Systems*, L. B. Rowell and J. T. Sheperd, Eds: Amer. Physiolog. Soc., 1996, pp. 173–216.

[13] A. H. Cohen, "The role of heterarchical control in the evolution of central pattern generators," *Brain Behav. Evol.*, vol. 40, pp. 112–124, 1992.

[14] S. Grillner and P. Wallen, "Central pattern generators for locomotion, with special reference to vertebrates," *Ann. Rev. Neurosci.*, vol. 8, pp. 233–261, 1985.

[15] S. Grillner, P. Wallén, and L. Brodin, "Neuronal network generating locomotor behavior in lamprey: Circuitry, transmitters, membrane properties, and simulation," *Ann. Rev. Neurosci.*, vol. 14, pp. 169–199, 1991.
[16] H. Barbeau and S. Rossignol, "Enhancement of locomotor recovery following spinal cord injury," *Curr. Opin. Neurol.*, vol. 7, pp. 517–524, 1994.
[17] V. Dietz, G. Colombo, L. Jensen, and L. Baumgartner, "Locomotor capacity of spinal cord in paraplegic patients," *Ann. Neurol.*, vol. 37, pp. 574–582, 1995.
[18] S. F. Giszter, F. A. Mussa-Ivaldi, and E. Bizzi, "Convergent force fields organized in the frog's spinal cord," *J. Neurosci.*, vol. 13, pp. 467–491, 1993.
[19] M. C. Tresch and E. Bizzi, "Responses to spinal microstimulation in the chronically spinalized rat and their relationship to spinal systems activated by low threshold cutaneous stimulation," *Exp. Brain Res.*, vol. 129, pp. 401–416, 1999.
[20] M. A. Lemay and W. M. Grill, "Endpoint forces evoked by microstimulation of the cat spinal cord," in 21st Annu. Int. Conf. IEEE/Engineering in Medicine and Biology Society Annu. Fall Meeting Biomedical Engineering Society, Atlanta, GA, 1999.
[21] F. A. Mussa-Ivaldi, S. F. Giszter, and E. Bizzi, "Linear combinations of primitives in vertebrate motor control," in *Proc. Natl. Acad. Sci. USA*, vol. 91, 1994, pp. 7534–7538.
[22] L. J. Calow and R. M. Alexander, "A mechanical analysis of a hind leg of a frog (*rana temporaria*)," *J. Zool. (London)*, vol. 171, pp. 293–321, 1973.
[23] J. B. Ranck, "Extracellular stimulation," in *Electrical Stimulation Research Techniques*, M. M. Patterson and R. P. Kesner, Eds. New York: Academic, 1981, pp. 2–34.
[24] J. S. Yeomans, *Principles of Brain Stimulation*. Oxford, U.K.: Oxford Univ. Press, 1990.
[25] P. E. Crago, P. H. Peckham, and G. B. Thrope, "Modulation of muscle force by recruitment during intramuscular stimulation," *IEEE Trans. Biomed. Eng.*, vol. BE-27, pp. 679–684, Dec. 1980.
[26] P. H. Gorman and J. T. Mortimer, "The effect of stimulus parameters on the recruitment characteristics of direct nerve stimulation," *IEEE Trans. Biomed. Eng.*, vol. BE-30, pp. 407–414, July 1983.
[27] E. Batschelet, *Circular Statistics in Biology*. New York: Academic, 1981.
[28] J. E. Galagan, M. A. Lemay, E. P. Loeb, and E. Bizzi, "EMG activity during vector summation of spinal force fields primitives," in 27th Annu. Meeting Soc. Neuroscience, New Orleans, LA, 1997.
[29] J. H. Lawrence and C. J. De Luca, "Myoelectric signal versus force relationship in different human muscles," *J. Appl. Physiol.*, vol. 54, pp. 1653–1659, 1983.
[30] J. Perry and G. A. Bekey, "EMG-force relationships in skeletal muscle," *Critic. Rev. Biomed. Eng.*, vol. 7, pp. 1–22, 1981.
[31] P. F. Gardiner, "Physiological properties of motoneurons innervating different muscle unit types in rat gastrocnemius," *J. Neurophysiol.*, vol. 69, pp. 1160–1170, 1993.
[32] Z.-P. Fang and J. T. Mortimer, "A method to effect physiological recruitment order in electrically activated muscle," *IEEE Trans. Biomed. Eng.*, vol. 38, pp. 174–179, 1991.
[33] V. K. Mushahwar and K. W. Horch, "Muscle recruitment through electrical stimulation of the lumbo-sacral spinal cord," *IEEE Trans. Rehab. Eng.*, vol. 8, pp. 22–29, Mar. 2000.
[34] C. Tai, A. M. Booth, C. J. Robinson, W. C. de Groat, and J. R. Roppolo, "Isometric torque about the knee joint generated by microstimulation of the cat L6 spinal cord," *IEEE Trans. Rehab. Eng.*, vol. 7, pp. 46–55, Mar. 1999.
[35] F. E. Zajac, M. R. Zomlefer, and W. S. Levine, "Hindlimb muscular activity, kinetics and kinematics of cats jumping to their maximum achievable heights," *J. Exp. Biol.*, vol. 91, pp. 73–86, 1981.
[36] S. E. Peters, L. T. Kamel, and D. P. Bashor, "Hopping and swimming in the leopard frog, Rana pipiens—I: Step cycles and kinematics," *J. Morphol.*, vol. 230, pp. 1–16, 1996.
[37] D. J. Ostry, A. G. Feldman, and J. R. Flanagan, "Kinematics and control of frog hindlimb movements," *J. Neurophysiol.*, vol. 65, pp. 547–562, 1991.
[38] H. Hultborn and O. Kiehn, "Neuromodulation of vertebrate motor neuron membrane properties," *Curr. Opin. Neurobiol.*, vol. 2, pp. 770–775, 1992.
[39] E. P. Zehr and R. B. Stein, "What functions do reflexes serve during human locomotion?," *Prog. Neurobiol.*, vol. 58, pp. 185–205, 1999.
[40] H. Barbeau, D. A. McCrea, M. J. O'Donovan, S. Rossignol, W. M. Grill, and M. A. Lemay, "Tapping into spinal circuits to restore motor function," *Brain Res. Rev.* , vol. 30, pp. 27–51, 1999.
[41] C. Tai, A. M. Booth, C. J. Robinson, W. C. de Groat, and J. R. Roppolo, "Multimicroelectrode stimulation within the cat L6 spinal cord: Influences of electrode combinations and stimulus interleave time on knee joint extension torque," *IEEE Trans. Rehab. Eng.*, vol. 8, pp. 1–10, Mar. 2000.
[42] P. Saltiel, M. C. Tresch, and E. Bizzi, "Spinal cord modular organization and rhythm generation: An NMDA iontophoretic study in the frog," *J. Neurophysiol.*, vol. 80, pp. 2323–2339, 1998.
[43] E. Bizzi, F. A. Mussa-Ivaldi, and S. Giszter, "Computations underlying the execution of movement: A biological perspective," *Sci.*, vol. 253, pp. 287–291, 1991.
[44] C. S. Sherrington, "Flexion-reflex of the limb, crossed extension reflex and reflex stepping and standing," *J. Physiol.*, vol. 40, pp. 28–121, 1910.
[45] R. E. Burke, "Movement programs in the spinal cord (ommentary)," *Behav. Brain Sci.*, vol. 15, p. 722, 1992.
[46] G. Szekely, "The morphology of motoneurons and dorsal root fibers in the frog's spinal cord," *Brain Res.*, vol. 103, pp. 275–290, 1976.
[47] E. P. Loeb, S. F. Giszter, P. Borghesani, and E. Bizzi, "Effects of dorsal root cut on the forces evoked by spinal microstimulation in the spinalized frog," *Somatosens. Mot. Res.*, vol. 10, pp. 81–95, 1993.
[48] V. K. Mushahwar and K. W. Horch, "Selective activation of muscle groups in the feline hindlimb through electrical microstimulation of the ventral lumbo-sacral spinal cord," *IEEE Trans. Rehab. Eng.*, vol. 8, pp. 11–21, Mar. 2000.
[49] J. I. Simpson, "Functional synaptology of the spinal cord," in *Frog Neurobiology. A Handbook*, R. L. A. W. Precht, Ed. Berlin: Springer-Verlag, 1976, pp. 728–749.
[50] M. R. Dimitrijevic, Y. Gerasimenko, and M. M. Pinter, "Evidence for a spinal central pattern generator in humans," *Ann. NY Acad. Sci.*, vol. 860, pp. 360–376, 1998.
[51] C. Tai, A. M. Booth, W. C. de Groat, C. Robinson, and J. R. Roppolo, "Coordinated hindlimb movement characterized by changes in angle at multiple joints produced by microstimulation of the lumbar cord in cat," in 30th Annu. Meeting Soc. Neuroscience, New Orleans, LA, 2000.
[52] M. A. Lemay, J. E. Galagan, E. Bizzi, and N. Hogan, "Attractor trajectory of spinal force field," in 28th Annu. Meeting Soc. Neuroscience, Los Angeles, CA, 1998.
[53] V. K. Mushawar and A. Prochazka, "Spinal cord microstimulation: Long-term stability of implanted microwires," in 29th Annu. Meeting Soc. Neuroscience, Miami, FL, 1999.
[54] F. A. Mussa-Ivaldi, "Nonlinear force fields: A distributed system of control primitives for representing and learning movements," in 1997 IEEE Int. Symp. on Computational Intelligence in Robotics and Automation , 1997, p. 84—90.
[55] B. J. Woodford, R. R. Carter, D. McCreery, L. A. Bullara, and W. F. Agnew, "Histopathologic and physiologic effects of chronic implantation of microelectrodes in sacral spinal cord of the cat," *J. Neuropathol. Exp. Neurol.*, vol. 55, pp. 982–991, 1996.

Michel A. Lemay (S'94–M'95) received the B.S. degree in electrical engineering from Sherbrooke University, Sherbrooke, Canada, in 1987 and the M.S. and Ph.D. degrees in biomedical engineering from Case Western Reserve University (CWRU), Cleveland, OH, in 1991 and 1994, respectively.

In 1998, he joined CWRU as a Senior Research Associate. In 2001, he joined the Neurobiology and Anatomy faculty as an Assistant Professor at MCP Hahnemann University, Philadelphia, PA. His research interests are in neural engineering and microstimulation of the spinal cord to restore coordinated movements.

Dr. Lemay is a member of the IEEE Engineering in Medicine and Biology Society, the Society for Neuroscience, the International FES Society, and l'Ordre des Ingenieurs du Quebec.

James E. Galagan received the B.S. degree in computer science and engineering from the University of California, Davis, and the Ph.D. degree in computational neuroscience from the Massachusetts Institute of Technology (MIT), Cambridge, MA, in 1992 and 1999, respectively.

In 1999, he joined Whitehead/MIT Center for Genome Research, where he is currently Team Leader of Annotation and Analysis Informatics. His research interests include computational methods for biological sequence analysis and comparative genomics.

Neville Hogan was born in Ireland. In 1970, he received the Diploma in engineering (with distinction) from the College of Technology, Dublin, Ireland, and received the M.S. and Ph.D. degrees in mechanical engineering from the Massachusetts Institute of Technology (MIT), Cambridge, in 1973 and 1977, respectively.

In 1979, he joined The Institute of Technology at MIT as a Faculty Member. Currently, he is a Professor of mechanical engineering and brain and cognitive sciences, and Director of the Newman Laboratory for Biomechanics and Human Rehabilitation. His research interests include robotics, biomechanics, and neural control of movement, emphasizing contact tasks and tool use applications include arm amputation prostheses, robotics, telerobotics, haptic virtual environment, and human performance enhancement technologies.

Emilio Bizzi was born in Rome, Italy. He received the M.D. degree from the University of Rome, Italy, in 1958 and the Docenza (the Italian equivalent of Ph.D.) in 1968.

He is currently the Eugene McDermott Professor in the Brain Sciences and Human Behavior at Massachusetts Institute of Technology (MIT). He served as Chairman of the Department of Brain and Cognitive Sciences at MIT from 1986 to 1997 and Director of Whitaker College of Health Sciences, Technology, and Management MIT from 1983 to 1989. He is a renowned Neuroscientist whose early career work included a study of the neurophysiological mechanism of sleep. Later, he investigated the sensory and motor events subserving the coordination between the eyes and the head. He has authored numerous publications over the years, including textbooks, journal articles, reviews and abstracts. His current research focuses on a series of investigations directed at understanding the learning of motor skills. His investigations have dealt with the mechanisms whereby the central nervous system simultaneously controls the large number of degrees of freedom of the multijoint musculo–skeletal system and the nature of the interaction between motor programs and afferent feedback. Recently, he and his collaborators provided evidence showing that the neural circuits in the spinal cord are organized into a number of distinct functional modules.

Dr. Bizzi is a member of the National Academy of Sciences (1986) and the American Academy of Arts and Sciences (1980), where he currently serves as Secretary. He has won awards for his research and academic work including the W. Alden Spencer Award and Hermann von Helmoltz Award for Excellence in Neuroscience. He serves on many committees and editorial boards, and is a Trustee of the Neuroscience Research Foundation.